

# Superfluidity in Three-species Mixture of Lithium Gases across Feshbach Resonances

Hui Zhai

Department of Physics, the Ohio-State University, Columbus, 43210, OH

(Dated: February 8, 2020)

In this letter we study the phase diagram and the properties of the superfluid phase in a mixture of the lowest three hyperfine spin states of lithium, within a particular range of magnetic field where two Feshbach resonances are close to each other. In the BEC side of two resonances the system is a binary mixture of molecular condensates, which undergoes a crossover to a superfluid containing two kinds of Cooper pairs as approaching resonances. Some remarkable properties, as well as the experimental consequences, of this superfluid phase are discussed. A quantum phase transition to the normal state is predicted at the BCS sides of two resonances, and the phase separation instability is also discussed.

*Introduction.* During the last few years, one of the major progresses in the cold atom physics is the achievement of superfluidity in the two-species mixture of fermionic lithium and potassium gases. The access of the superfluid phase in the gaseous system relies on Feshbach resonances, across which the system undergoes a crossover from BCS to BEC and the transition temperature can be as high as the same order of magnitude of the Fermi temperature. Recently the scattering lengths between the lowest three hyperfine spin states of lithium, denoted as  $|1\rangle$ ,  $|2\rangle$  and  $|3\rangle$  respectively, have been measured precisely for a wide range of magnetic field[1], and two broad Feshbach resonances between  $|1\rangle - |2\rangle$  and between  $|2\rangle - |3\rangle$  are found close to each other with the magnetic field located at  $81.1\text{mT}$  and  $83.4\text{mT}$  respectively, as shown in Fig.1. This creates the opportunity to study the fermion pairing and superfluidity in the three-species mixture experimentally in the nearly future. Recently, there are also several theoretical papers appearing to address the physics of three-species mixture[2, 3, 4, 5], however, most of them are in the weakly-interacting regime. It is the subject of this letter to present an microscopic many-body theory, which takes the physics of Feshbach resonance and the actual scattering properties of lithium atoms into account.

Note that both the  $|1\rangle - |2\rangle$  molecule and the  $|2\rangle - |3\rangle$  molecule are stable at the BEC sides of two resonances, a condensates of the binary mixture of these two molecules will imply that the numbers of fermionic atoms satisfy  $N_2 = N_1 + N_3$ . In this work we shall limit our study of crossover physics to this case, and the content of this letter includes (i) generalizing the mean-field theory for BEC-BCS crossover[6] to two-component BEC, which describes how the system undergoes a crossover to a superfluid with two kinds of Cooper pairs; (ii) discussing how the ground state evolves as magnetic field changes, and constructing the phase diagram which is summarized in Fig.1 and its caption; and (iii) pointing out some unique properties and experimental signatures of this two-component superfluid state.

*Mean-field Theory of Two-component Superfluid.* Following the idea of crossover theory, we write down a BCS-

like wave function which contains pairing between both  $|1\rangle - |2\rangle$  and  $|2\rangle - |3\rangle$  [7]

$$|\Psi\rangle = \prod_{\mathbf{k}} \left( u_{\mathbf{k}} + v_{\mathbf{k}} \psi_{\mathbf{k}2}^\dagger \psi_{-\mathbf{k}1}^\dagger + w_{\mathbf{k}} \psi_{\mathbf{k}2}^\dagger \psi_{-\mathbf{k}3}^\dagger \right) |0\rangle. \quad (1)$$

We neglect the pairing between  $|1\rangle - |3\rangle$  because their interaction is weak in the range of magnetic field from  $78\text{mT}$  to  $88\text{mT}$ , comparing to those between  $|1\rangle - |2\rangle$  and between  $|2\rangle - |3\rangle$ [1]. Therefore, for energetic consideration both of  $|1\rangle$  and  $|3\rangle$  try to pair with  $|2\rangle$  first, and also the critical temperature for  $|1\rangle - |3\rangle$  pairing instability is too low to reach in current experiments.

Before proceeding, we would like to emphasize the order parameters and symmetry breaking properties of this state. First, there are two independent pairing order pa-

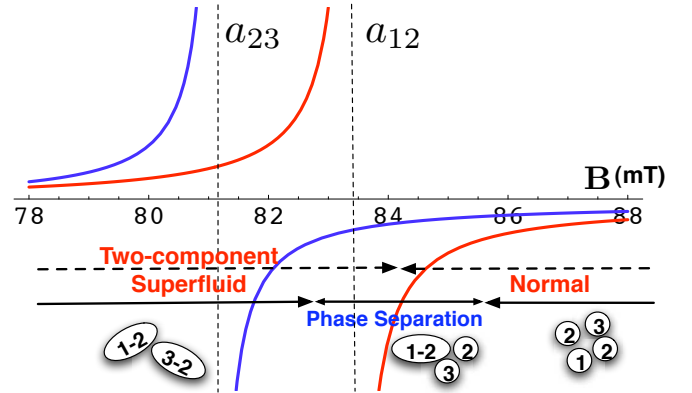


FIG. 1: An illustration of the scattering lengths  $a_{12}$  and  $a_{23}$  as a function of magnetic field and the phase diagram for the three-species mixture with  $N_2 = N_1 + N_3$ . The relation between scattering length and magnetic field is found from Ref.[1]. In this range of magnetic field  $a_{23}$  is negative and relatively small, and it is not shown here. Restricted in homogeneous states, a first order quantum phase transition form the two-component superfluid state to the normal state is found above the first resonance. Incorporating inhomogeneous states, the phase separated state will take over around the critical magnetic field. The locations of phase boundary will depend on the density and the concentration.

rameters,  $\Delta_1 = \langle \psi_2^\dagger \psi_1^\dagger \rangle$  and  $\Delta_2 = \langle \psi_2^\dagger \psi_3^\dagger \rangle$ . Furthermore, as both species  $|1\rangle$  and  $|3\rangle$  pair with species  $|2\rangle$ , the operator  $\psi_3^\dagger \psi_1$ , which in fact converts a  $|2\rangle - |1\rangle$  pair into a  $|2\rangle - |3\rangle$  pair, acts as a Josephson tunneling between two components, and the wave function Eq.(1) automatically gives another order parameter  $\eta = \langle \psi_3^\dagger \psi_1 \rangle$  which is related to the relative phase between two components and determined by spontaneous symmetry breaking.

Focusing on this particular range of magnetic field, the Hamiltonian can be written as

$$\mathcal{H} = \sum_{\mathbf{k}\sigma} \epsilon_{\mathbf{k}\sigma} \psi_{\mathbf{k}\sigma}^\dagger \psi_{\mathbf{k}\sigma} + \sum_{\mathbf{k}, \mathbf{k}', i} g_{2i} \psi_{\mathbf{k}2}^\dagger \psi_{-\mathbf{k}i}^\dagger \psi_{-\mathbf{k}'i} \psi_{\mathbf{k}'2}, \quad (2)$$

where  $\epsilon_{\mathbf{k}\sigma} = \hbar^2 k^2 / (2m) - \mu_\sigma$ ,  $\sigma = 1, 2, 3$  and  $i = 1, 3$ . As in the two-species mixture,  $g_{2i}$  is related to the scattering lengths via  $1/g_{2i} = m / (4\pi \hbar^2 a_{2i}) - \sum_{\mathbf{k}} m / (\hbar^2 k^2)$ . Here we neglect the interaction between  $|1\rangle - |3\rangle$ , which can be turned on as perturbation in a more detailed study later. It will not affect the qualitative features discussed here.

With the Hamiltonian Eq.(2) the free-energy for the quantum state of Eq.(1) is given by

$$\mathcal{F} = \sum_{\mathbf{k}} (\xi_{\mathbf{k}a} |v_{\mathbf{k}}|^2 + \xi_{\mathbf{k}b} |w_{\mathbf{k}}|^2) + \sum_{\mathbf{k}\mathbf{k}'} g_{21} u_{\mathbf{k}} v_{\mathbf{k}}^* u_{\mathbf{k}'}^* v_{\mathbf{k}'} + g_{23} u_{\mathbf{k}} w_{\mathbf{k}}^* u_{\mathbf{k}'}^* w_{\mathbf{k}'}, \quad (3)$$

where  $\xi_{\mathbf{k}a} = \epsilon_{\mathbf{k}1} + \epsilon_{\mathbf{k}2}$  and  $\xi_{\mathbf{k}b} = \epsilon_{\mathbf{k}2} + \epsilon_{\mathbf{k}3}$ . The constraint  $|u_{\mathbf{k}}|^2 + |v_{\mathbf{k}}|^2 + |w_{\mathbf{k}}|^2 = 1$  can be imposed by a Langrange multiplier  $\sum_{\mathbf{k}} \lambda_{\mathbf{k}} (|u_{\mathbf{k}}|^2 + |v_{\mathbf{k}}|^2 + |w_{\mathbf{k}}|^2 - 1)$ . The condition for free-energy minimum is given by  $\partial \mathcal{F} / \partial u_{\mathbf{k}} = \partial \mathcal{F} / \partial v_{\mathbf{k}} = \partial \mathcal{F} / \partial w_{\mathbf{k}} = 0$ , which are

$$\begin{pmatrix} \lambda_{\mathbf{k}} & \Delta_1 & \Delta_2 \\ \Delta_1^* & \lambda_{\mathbf{k}} - \xi_{\mathbf{k}a} & 0 \\ \Delta_2^* & 0 & \lambda_{\mathbf{k}} - \xi_{\mathbf{k}b} \end{pmatrix} \begin{pmatrix} u_{\mathbf{k}} \\ v_{\mathbf{k}} \\ w_{\mathbf{k}} \end{pmatrix} = 0, \quad (4)$$

where  $\Delta_1 = -g_{21} \sum_{\mathbf{k}} u_{\mathbf{k}} v_{\mathbf{k}}^*$  and  $\Delta_2 = -g_{23} \sum_{\mathbf{k}} u_{\mathbf{k}} w_{\mathbf{k}}^*$ . Thus  $\lambda_{\mathbf{k}}$  satisfies the equation  $\lambda_{\mathbf{k}}^3 - A_{\mathbf{k}} \lambda_{\mathbf{k}}^2 + B_{\mathbf{k}} \lambda_{\mathbf{k}} + C_{\mathbf{k}} = 0$ , where  $A_{\mathbf{k}} = \xi_{\mathbf{k}a} + \xi_{\mathbf{k}b}$ ,  $B_{\mathbf{k}} = \xi_{\mathbf{k}a} \xi_{\mathbf{k}b} - |\Delta_1|^2 - |\Delta_2|^2$  and  $C_{\mathbf{k}} = |\Delta_1|^2 \xi_{\mathbf{k}b} + |\Delta_2|^2 \xi_{\mathbf{k}a}$ . The lowest solution to this cubic equation is  $\lambda_{\mathbf{k}} = \{A_{\mathbf{k}} - 2\sqrt{A_{\mathbf{k}}^2 - 3B_{\mathbf{k}}} \cos[(\pi - \theta_{\mathbf{k}})/3]\}/3$ , where  $\theta_{\mathbf{k}} = \arctan[3\sqrt{3}K_{\mathbf{k}}/(2A_{\mathbf{k}}^3 - 9A_{\mathbf{k}}B_{\mathbf{k}} - 27C_{\mathbf{k}})]$  and  $K_{\mathbf{k}} = A_{\mathbf{k}}^2 B_{\mathbf{k}}^2 - 4B_{\mathbf{k}}^3 + 4A_{\mathbf{k}}^3 C_{\mathbf{k}} - 18A_{\mathbf{k}}B_{\mathbf{k}}C_{\mathbf{k}} + 27C_{\mathbf{k}}^2$ [8].

For the wave function satisfying Eq.(4), the free-energy is given by  $\mathcal{F} = \sum_{\mathbf{k}} \lambda_{\mathbf{k}} - |\Delta_1|^2 / g_{21} - |\Delta_2|^2 / g_{23}$ . It can be verified that the long wave length behavior of  $\lambda_{\mathbf{k}}$  is precisely  $-(|\Delta_1|^2 + |\Delta_2|^2)m / (\hbar^2 k^2)$ , therefore the divergency in the summation over  $\lambda_{\mathbf{k}}$  can be exactly canceled out by a proper renormalization of  $g_{21}$  and  $g_{23}$ . Furthermore, we know that  $\partial \mathcal{F} / \partial \Delta_1^* = 0$  can lead to a self-consistency equation for  $\Delta_1$ , and by noticing that  $\lambda_{\mathbf{k}}$  satisfies the cubic equation, we have

$$(3\lambda_{\mathbf{k}}^2 - 2A_{\mathbf{k}}\lambda_{\mathbf{k}} + B_{\mathbf{k}}) \frac{\partial \lambda_{\mathbf{k}}}{\partial \Delta_1^*} = \Delta_1 (\lambda_{\mathbf{k}} - \xi_{\mathbf{k}b}). \quad (5)$$

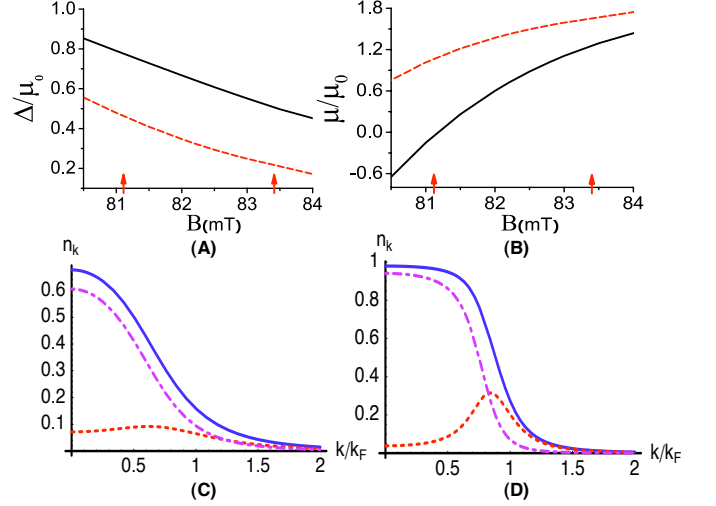


FIG. 2: The solution to the mean-field equations. (A-B): As the change of magnetic field, the evolvement of two pairing order parameters  $\Delta_1$  (solid line) and  $\Delta_2$  (dashed line) (Fig.A), and the chemical potential  $\mu_a = \mu_1 + \mu_2$  (solid line) and  $\mu_b = \mu_2 + \mu_3$  (dashed line) (Fig.B). (C-D): The momentum distributions for  $|1\rangle$  (dashed line),  $|2\rangle$  (solid line) and  $|3\rangle$  (dashed-dotted line) at  $80.5mT$  (Fig.C) and  $84mT$  (Fig.D). Here we have chosen  $n_2 = 1.14 \times 10^{11} \text{ cm}^{-3}$  and  $N_2 : N_1 : N_3 = 1 : 0.5 : 0.5$ . The two arrows in (A) and (B) indicate the locations of Feshbach resonances.  $k_F$  is the Fermi momentum for the majority species  $|2\rangle$ , and  $\mu_0 = \hbar^2 k_F^2 / (2m)$ .

Thus, it yields that

$$\frac{m}{4\pi \hbar^2 a_{12}} = \sum_{\mathbf{k}} \left( \frac{\lambda_{\mathbf{k}} - \xi_{\mathbf{k}b}}{3\lambda_{\mathbf{k}}^2 - 2A_{\mathbf{k}}\lambda_{\mathbf{k}} + B_{\mathbf{k}}} + \frac{1}{\hbar^2 k^2 / m} \right). \quad (6)$$

And similarly we can obtain another equation as

$$\frac{m}{4\pi \hbar^2 a_{23}} = \sum_{\mathbf{k}} \left( \frac{\lambda_{\mathbf{k}} - \xi_{\mathbf{k}a}}{3\lambda_{\mathbf{k}}^2 - 2A_{\mathbf{k}}\lambda_{\mathbf{k}} + B_{\mathbf{k}}} + \frac{1}{\hbar^2 k^2 / m} \right). \quad (7)$$

Apart from the gap equations, another major effect of the BEC-BCS crossover is the renormalization of chemical potentials, which is determined by the number equations. From Eq.(4) we can get  $u_{\mathbf{k}}/v_{\mathbf{k}} = (\xi_{\mathbf{k}a} - \lambda_{\mathbf{k}})/\Delta_1^*$  and  $w_{\mathbf{k}}/v_{\mathbf{k}} = [\lambda_{\mathbf{k}}(\lambda_{\mathbf{k}} - \xi_{\mathbf{k}a}) - |\Delta_1|^2]/(\Delta_1^* \Delta_2)$ . Therefore, two number equations are given by  $N_1 = \sum_{\mathbf{k}} |v_{\mathbf{k}}|^2 = \sum_{\mathbf{k}} (1/(1 + |u_{\mathbf{k}}/v_{\mathbf{k}}|^2 + |w_{\mathbf{k}}/v_{\mathbf{k}}|^2))$  and  $N_3 = \sum_{\mathbf{k}} |w_{\mathbf{k}}|^2 = \sum_{\mathbf{k}} (|w_{\mathbf{k}}/v_{\mathbf{k}}|^2 / (1 + |u_{\mathbf{k}}/v_{\mathbf{k}}|^2 + |w_{\mathbf{k}}/v_{\mathbf{k}}|^2))$  respectively.

We solve these four joint equations numerically, and the results are shown in Fig.2, which exhibit the common features of BEC-BCS crossover. From Fig.2(A-B), one can see that the gaps increase and the chemical potentials decrease as the magnetic field changes from the BCS side to BEC side[9]. It is also noticed that both the two gaps and the two chemical potentials are different from each other, even although  $N_1 = N_3$ , simply because

the attraction between  $|2\rangle - |1\rangle$  is always stronger than that between  $|2\rangle - |3\rangle$ . In Fig.2(C-D) we also plot the momentum distributions for three different species. One can see that the momentum distributions become much broader at the BEC side than at the BCS side, which indicates that the sizes of two kinds of Cooper pairs in real space shrink as the decrease of magnetic field. Furthermore, this solution also allows to calculate the energy of this superfluid state  $E_{\text{SF}}$ .

*Quantum Phase Transition for Homogeneous System.* It is noticed that in the normal state the Fermi surface of species  $|2\rangle$  is larger than those of species  $|1\rangle$  and  $|3\rangle$  for the concentration  $N_2 = N_1 + N_3$ , therefore in the BCS side it will cost a lot of kinetic energy of two minority species to pair with the majority species. As one can see from Fig.2(D), the momentum distribution for species  $|1\rangle$  has to deform a lot comparing to its normal state. Therefore, one expect that there is a quantum phase transition from this two-component superfluid state to the normal state as approaching weakly-interacting BCS side.

At mean-field level, we simply take the normal state as non-interacting normal state, and its energy  $E_N$  is just the total kinetic energy of three species. In Fig.3(A-B) we plot the energy difference  $\delta E = E_N - E_{\text{SF}}$  for different densities and concentrations. A quantum phase transition occurs when  $\delta E$  becomes negative, i.e. the normal state has lower energy, which is usually located above the first Feshbach resonance, while the exact location of the critical field depends on both the density and the concentration. From the figure we find that the critical magnetic field will be pushed toward the BCS side either when the density of atoms increases or when the ratio  $N_1 : N_3$  increases[10]. We also notice that there is no continuous route to connect the quantum states of the form Eq.(1) with a normal state, therefore this transition should be a first order quantum phase transition.

*Phase Separation Instability.* Intuitively speaking, there are two types of possible phase separation instability, and now we will compare their energy with homogeneous states. From an alternative view of the normal state, the mixture of species  $|1\rangle$  and  $|2\rangle$  by themselves is a mixture with unequal population and polarization  $P = (N_2 - N_1)/(N_2 + N_1)$ . When the attraction between  $|1\rangle - |2\rangle$  becomes strong, the energy will be lowered if the mixture phase separates into a superfluid with equal population and the excess majority species [11, 12]. According to this, here we construct a phase separated state, in one region it is  $\prod_{\mathbf{k}}(u_{\mathbf{k}} + v_{\mathbf{k}}\psi_{\mathbf{k}2}^\dagger\psi_{-\mathbf{k}1}^\dagger)\prod_{\mathbf{p}=0}^{p_F}\psi_{\mathbf{p}3}^\dagger|0\rangle$  and in another region it is  $\prod_{\mathbf{k}=0}^{k_F}\psi_{\mathbf{k}2}^\dagger\prod_{\mathbf{p}=0}^{p_F}\psi_{\mathbf{p}3}^\dagger|0\rangle$ , and the energy of this state is shown in Fig.3(C) for a typical density and concentration, comparing with the energy of the homogeneous states. We find that around the critical magnetic field the energy of phase separated state is lower than both two homogeneous states.

In the two-component superfluid phase, we first need

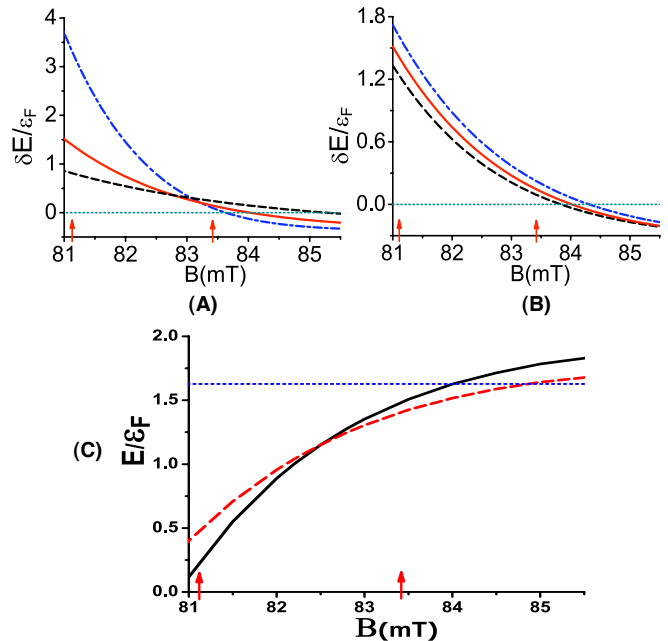


FIG. 3: (A-B)  $\delta E$  as a function of magnetic field. (A):  $N_2 : N_1 : N_3 = 1 : 0.5 : 0.5$  and  $k_F a_0 = 1 \times 10^{-4}$  (solid line),  $k_F a_0 = 0.5 \times 10^{-4}$  (dashed line),  $k_F a_0 = 2 \times 10^{-4}$  (dashed-dotted line). (B)  $k_F a_0 = 1 \times 10^{-4}$  and  $N_2 : N_1 : N_3 = 1 : 0.5 : 0.5$  (solid line),  $N_2 : N_1 : N_3 = 1 : 0.4 : 0.6$  (dashed line),  $N_2 : N_1 : N_3 = 1 : 0.6 : 0.4$  (dashed-dotted line). (C) Comparison of the energy between the phase separated state (dashed line), the two-component superfluid state (solid line) and the normal state (dotted line).  $k_F a_0 = 1 \times 10^{-4}$  and  $N_2 : N_1 : N_3 = 1 : 0.5 : 0.5$ . For all figures the unit of energy density is  $\mathcal{E}_F = \hbar^2 k_F^3 / (20\pi^2 m)$ ,  $k_F$  is the Fermi momentum of the major species  $|2\rangle$  in its normal state, and  $a_0 = 0.0529177\text{nm}$ . Two arrows indicate the locations of Feshbach resonances.

to find out the sign of the effective interaction between unlike molecules. We calculate the quantity  $\kappa = \partial^2 \mathcal{F} / (\partial |\Delta_1|^2 \partial |\Delta_2|^2) = \sum_{\mathbf{k}} \partial \lambda_{\mathbf{k}}^2 / (\partial |\Delta_1|^2 \partial |\Delta_2|^2)$ , and we find that  $\kappa$  is always positive, which indicates the interaction to be repulsive. Hence, one need to consider whether this two-component condensate will spatially separate into two condensates, with  $|2\rangle - |1\rangle$  molecules staying in one side and  $|2\rangle - |3\rangle$  molecules staying in another side, in case the repulsion between unlike molecules are too strong. Here we also calculate the energy of this type phase separated state, and find that the energy is very close to, but usually slightly higher than, the energy of the homogeneous state in all range of magnetic field. Thus we conclude that this separation will not happen.

Combining the discussion on the homogeneous states and the phase separation instability, we draw the conclusion on the phase diagram illustrated in Fig.1.

*Experimental Signatures of the Two-component Superfluid.* Here we would like to stress again that the quantum state of Eq.(1) emerged from the three-species mix-

ture is a new type of superfluid state, and has many unique properties, which will show up in a lot of experimental measurements and distinguish this state from the normal state and the conventional superfluid state.

Radio-frequency spectroscopy, which can be described by the Hamiltonian such as  $H_{\text{rf}} = \psi_3^\dagger \psi_1 + \text{h.c.}$ , has been used as a powerful tool in fermion experiments[13, 14]. In the two-species mixture, the r-f field will cause loss of atoms in species  $|1\rangle$ , and from the loss fraction one can read out the information on the mean-field energy of normal state[13] and the pairing gap of superfluid state[14]. Here, as pointed out at the beginning, the operator  $\psi_3^\dagger \psi_1$  plays a role as internal Josephson coupling between two superfluid order parameters. Thus, rather than loss of atoms, applying r-f field will induce a time-periodic oscillation of the atom number in both species  $|1\rangle$  and  $|3\rangle$ .

In the harmonic trap, the density profile of atoms now can be measured *in situ* with high accuracy[12]. A direct signal to distinguish this state from the normal state is that the density profile of different species have to satisfy  $n_2(\mathbf{r}) = n_1(\mathbf{r}) + n_3(\mathbf{r})$  everywhere, and the Thomas-Fermi radii are the same for all species. In contrast, in the normal state the Thomas-Fermi radius of the majority species is larger than those of two minority species, and  $n_2(\mathbf{r})$  does not equal to  $n_1(\mathbf{r}) + n_3(\mathbf{r})$  everywhere. For example, we calculate the column density  $n(r) = \int dz n(\mathbf{r})$  for non-interacting normal state, and at the center of the trap,  $n_2/(n_1 + n_3) = N_2^{2/3}/(N_1^{2/3} + N_3^{2/3}) < 1$ .

Analyzing the noise correlation in time-of-flight image allows to measure the correlation function  $\mathcal{G}_{\alpha\beta}(\mathbf{k}, \mathbf{k}') = \langle \hat{n}_{\alpha\mathbf{k}} \hat{n}_{\beta\mathbf{k}'} \rangle - \langle \hat{n}_{\alpha\mathbf{k}} \rangle \langle \hat{n}_{\beta\mathbf{k}'} \rangle$ [15]. In this state  $\mathcal{G}_{21}(\mathbf{k}, \mathbf{k}') = |u_{\mathbf{k}} v_{\mathbf{k}}|^2 \delta(\mathbf{k} + \mathbf{k}')$  and  $\mathcal{G}_{23}(\mathbf{k}, \mathbf{k}') = |u_{\mathbf{k}} w_{\mathbf{k}}|^2 \delta(\mathbf{k} + \mathbf{k}')$ , which shows strong pairing correlation between opposite momentums. Here, one unique feature is the effective exclusive correlation between  $|1\rangle$  and  $|3\rangle$ , and it shows up in  $\mathcal{G}_{13}(\mathbf{k}, \mathbf{k}') = -|v_{\mathbf{k}} w_{\mathbf{k}}|^2 \delta(\mathbf{k} - \mathbf{k}')$  which has a dip at equal momentum. This arises from the fact that the atom in the quantum state  $|2, -\mathbf{k}\rangle$  can only pair with either  $|1, \mathbf{k}\rangle$  or  $|3, \mathbf{k}\rangle$ , thus the quantum state with momentum  $\mathbf{k}$  can not be occupied by both  $|1\rangle$  and  $|3\rangle$ .

*Discussions.* The experimental concern of achieving superfluid phase is the three-body loss rate. In contrast to the two-species mixture which is stabilized by the Pauli exclusion principle, here the Pauli principle can only help to suppress the inelastic collision between molecules, but it can not suppress the collision between a molecule and a third species atom, which could be a dominating source of atom loss. So far we do not aware of any theoretical calculation or experimental date on the loss rate for this specific system, it is not clear how large it will be. However we know that the situation is not as worse as bosonic system, because not all the scattering lengths are very large at the same magnetic field. Besides, if the system is initially prepared deeply in the BEC side and

then tuned to the resonance regime, the loss rate may be reduced because there are few free atoms in the mixture.

There are a lot of questions remaining to further study. It is worth finding out how the relative phase fluctuation evolves across resonances, and it will be very unusual if the phase coherence is maintained deep in BEC side. The quantum fluctuations will also give corrections to the energy of the normal state and the superfluid state, which will quantitatively affect the phase diagram. Besides, depending on the ratio  $N_1 : N_3$ , the attraction between  $|1\rangle - |3\rangle$  may cause pairing instability in the normal state, although the transition temperature should be very low.

The author acknowledge Tin-Lun Ho for insightful discussion and helpful comments on the manuscript, Zuo-Zi Chen for numerical assistance and Cheng Chin for helpful discussion on the scattering properties of lithium. This work is supported by NSF Grant DMR-0426149 awarded to T.L.Ho.

- 
- [1] M. Bartenstein *et.al.* Phys. Rev. Lett. **94**, 103201 (2005)
  - [2] A. G. K. Modawi and A. J. Leggett, Jour. of . Low. Temp. Phys. **109**, 625 (1997)
  - [3] T. Paananen, J.-P. Martikainen, and P. Törmä, Phys. Rev. A **73**, 053606 (2006)
  - [4] P. F. Bedaque and J. P. D’Incao, cond-mat/0602525
  - [5] The three-body problem in a harmonic trap was recently solved by T. Luu and A. Schwenk, cond-mat/0606069
  - [6] A. J. Leggett in *Modern Trends in the Theory of Condensed Matter*, A. Pekalski and R. Przystawa, eds (Springer-Verlag, Berlin, 1980) and M. Randeria in *Bose-Einstein Condensation*, A. Griffin, D. W. Snoke and S. Stringari, eds(Cambridge University Press, 1995).
  - [7] This wave function can be written in an equivalent but more intuitive way as  $\prod_{\mathbf{p}}(\bar{u}_{\mathbf{p}} + \bar{v}_{\mathbf{p}} \Psi_{\mathbf{p}2}^\dagger \Psi_{-\mathbf{p}1}^\dagger) \prod_{\mathbf{q}}(\bar{u}_{\mathbf{q}} + \bar{v}_{\mathbf{q}} \Psi_{\mathbf{q}2}^\dagger \Psi_{-\mathbf{q}3}^\dagger)|0\rangle$ .
  - [8] Weisstein, Eric W. "Cubic Formula." From MathWorld—A Wolfram Web Resource. <http://mathworld.wolfram.com/CubicFormula.html>
  - [9] Following the terminology used in the discussion of two-species mixture, we call the high field regime as the BCS side and the low field regime as the BEC side.
  - [10] In the limit  $N_3 \rightarrow 0$ , the superfluid state will always has a lower energy than the normal state, which recovers the two-species mixture case.
  - [11] C.-H. Pao, S.-T. Wu, and S.-K. Yip, Phys. Rev. B **73**, 132506 (2006)
  - [12] M. W. Zwierlein, *et.al.* Science **311**, 492 (2006); G. B. Partridge, *et.al.* Science **311**, 503 (2006); M. W. Zwierlein, *et.al.* cond-mat/0605258 and Y. Shin, *et.al.* cond-mat/0606432
  - [13] S. Gupta, *et.al.* Science **300**,1723 (2003)
  - [14] C. Chin, *et.al.* Science, **305**, 1128 (2004) and J. Kinnunen, M. Rodriguez, and P. Törmä, Science, **305**, 1131 (2004).
  - [15] M. Greiner, *et.al.* Phys. Rev. Lett. **94**, 110401 (2005), E. Altman, *et.al.* Phys. Rev. A **70**, 013603 (2004).